Journal of Inflammation Research

Dovepress
open access to scientific and medical research

Open Access Full Text Article

ORIGINAL RESEARCH

Analyzing Immune Cell Infiltration and Copper Metabolism in Diabetic Foot Ulcers

Wen-Juan Yi[1,*], Yifan Yuan[2,*], Qionglin Bao[3], Zhuowei Zhao[4], Hua-Sheng Ding[5], Jiquan Song[1]

[1]Department of Dermatology, Zhongnan hospital of Wuhan University, Wuhan, People's Republic of China; [2]Center of Gerontology and Geriatrics, West China Hospital, Sichuan University, Chengdu, People's Republic of China; [3]Wound Repair Center, Chronic Wound and Diabetic Foot Clinical Medical Research Center, Liyuan Hospital Affiliated to Tongji Medical College, Huazhong University of Science and Technology, Wuhan, People's Republic of China; [4]Hubei Key Laboratory of Cell Homeostasis, College of Life Sciences, TaiKang Center for Life and Medical Sciences, Wuhan University, Wuhan, People's Republic of China; [5]Department of Emergency, Shenzhen Hospital, Southern Medical University, Shenzhen, People's Republic of China

*These authors contributed equally to this work

Correspondence: Hua-Sheng Ding; Jiquan Song, Email hsding2019@126.com; songjiq@126.com

Video abstract

Point your SmartPhone at the code above. If you have a QR code reader the video abstract will appear. Or use: https://youtu.be/11aoTmZYTjk

Background: Diabetes impairs wound healing, notably in diabetic foot ulcers (DFU). Stress, marked by the accumulation of lipoylated mitochondrial enzymes and the depletion of Fe–S cluster proteins, triggers cuproptosis—a distinct form of cell death. The involvement of copper in the pathophysiology of DFU has been recognized, and currently, a copper-based therapeutic strategy is emerging as a viable option for enhancing ulcer healing. This study investigates genes linked to copper metabolism in DFU, aiming to uncover potential targets for therapeutic intervention.

Methods: Two diabetic wound Gene Expression Omnibus (GEO) datasets were analyzed to study immune cell dysregulation in diabetic wounds. Differentially expressed genes related to copper metabolism were identified and analyzed using machine learning methods. Gene ontology, pathway enrichment, and immune infiltration analyses were performed using DFU samples. The expression of identified genes was validated using qRT-PCR and single-cell RNA sequencing.

Results: Ten genes associated with copper metabolism were identified. Among these, SLC31A1 and ADNP were found to be significantly differentially expressed in DFU. Notably, SLC31A1 exhibited higher expression in macrophages, whereas ADNP was found to be highly expressed in fibroblasts and chondrocytes.

Conclusion: The study indicates a close link between copper metabolism, the infiltration of immune cells, and DFU. It proposes that copper metabolism could influence the progression of DFU through the activation of immune responses. These observations offer fresh perspectives on the underlying mechanisms of DFU and identify potential targets for therapeutic intervention.

Keywords: diabetic foot ulcers, copper metabolism, immune infiltration, single-cell RNA analysis, differentially expressed genes

Introduction

Diabetes mellitus is a chronic metabolic disease characterized by prolonged high blood sugar levels, affecting an increasing number of individuals worldwide. Diabetic foot ulcer (DFU) is a common complication, which is essentially a chronic, difficult-to-heal wound. Approximately 20% of all diabetes patients experience impaired healing of foot ulcers and non-healing wounds, leading to lower limb amputations and high economic and psychosocial costs.[1] In diabetic wounds, the healing process is impeded by tissue ischemia, hypoxia, and a high-glucose microenvironment, leading to delayed or nonhealing wounds and numerous clinical complications.[2] The primary risk factors for DFU include peripheral neuropathy, which can manifest as sensory, motor, or autonomic dysfunctions, thereby elevating the risk of DFU development.[3] Despite the recognition of these risk factors, the intricate molecular mechanisms governing DFU healing remain elusive, highlighting the need for further research to enhance our understanding.

Received: 30 November 2023
Accepted: 18 April 2024
Published: 17 May 2024

A recent groundbreaking study by Tsvetkov P. introduced a newly discovered form of cell death called cuproptosis, which is specifically induced by copper toxicity.[4] Unlike other known cell death mechanisms such as apoptosis, necroptosis, autophagy, pyroptosis, and ferroptosis, cuproptosis operates through a distinct process involving the direct binding of copper ions to fatty acylated components of the tricarboxylic acid (TCA) cycle in mitochondrial respiration.[5] This binding leads to the aggregation of fatty acylated proteins, destabilization of Fe-S cluster proteins, increased proteotoxic stress, and ultimately cell death.[4,6] Mitochondria play a crucial role in regulating copper homeostasis as copper ions (Cu^{2+}) serve as cofactors for enzymes. Copper ionophores, which are small molecules that transport copper into cells, are used in research to investigate copper toxicity.[7] It should be noted that the mechanism by which copper ionophores induce cell death involves the accumulation of intracellular copper rather than the action of the ionophores themselves.

Previous studies indicate that DFU patients exhibit significantly lower serum copper levels compared to diabetics without ulcers, with these levels inversely correlating with glycaemic indices.[8,9] Copper plays a crucial role in wound healing processes, such as elastin and collagen crosslinking, angiogenesis promotion, and protection against free radicals, highlighting its importance in skin repair mechanisms.[10] Recent interest in copper dressings for DFU underlines copper's significant impact on wound recovery. Copper dressings enhance wound healing by upregulating pro-angiogenic factors like hypoxia-inducible factor-1 alpha and vascular endothelial growth factor, leading to increased blood vessel formation and improved wound closure.[10,11] The copper-based therapeutic strategy emerges as a viable option for enhancing ulcer healing, with the added benefit of copper's antimicrobial properties potentially lowering infection risks at the ulcer site, thus promoting further healing advancements. Therefore, it can be inferred that there is a strong correlation between copper metabolism and the pathophysiology of DFU. However, the exact mechanisms, particularly how copper interacts with immune infiltration, remain elusive.

To further investigate the mechanisms involved in diabetic wound pathogenesis, we conducted a rigorous analysis using the Gene Expression Omnibus (GEO) database. Our analysis focused on identifying genes that exhibit differential expression between normal and DFU samples. To ensure the accuracy of our findings, we employed multiple machine learning algorithms to identify critical differential genes. Additionally, we explored the relationship between copper metabolism and immune infiltration, providing a novel perspective to better understand the underlying molecular mechanisms involved in diabetic wound pathogenesis. Additionally, clinical samples were conducted to validate the expression profiles of copper metabolism-related genes (CMRGs) in skin tissues of DFU. Finally, we applied the single-cell analysis to confirm the correlation between copper metabolism and DFU.

Materials and Methods

The Acquisition of Datasets and CMRGs

We utilized the "GEOquery" R program to acquire two raw datasets, namely GSE29221 and GSE7014, from the GEO database (https://www.ncbi.nlm.nih.gov/geo/). These datasets contained gene expression data specifically focused on DFU and control subjects. The GSE29221 dataset comprised 12 DFU and 12 normal samples, and the GSE7014 dataset included 30 DFU and 6 control samples. To facilitate subsequent analyses, all the gene expression data was transformed into logarithmic form (log2). To ensure the elimination of any batch effects and to create a unified dataset from the GEO datasets, we employed the "sva" R software from the Bioconductor platform. We aimed to mitigate any potential biases introduced during data collection and processing. To identify genes associated with copper metabolism, we combined the copper metabolism genes available in the Molecular Signature Database (MsigDB) v7.0 (http://www.gsea-msigdb.org/gsea/msigdb/) with gene sets relevant to copper metabolism from a previous study. After removing any duplicates, we identified 52 CMRGs, which will be further examined in our subsequent analyses and investigations.

Identification of Differentially Expressed Genes (DEGs) and Candidate Key CMRGs

We employed the R package "limma" to conduct a differential gene analysis, aiming to identify DEGs between the illness and health samples. For this analysis, we established a significance threshold of adjusted $P<0.05$. We visually represented the DEGs data using volcano plots and heatmaps. The candidate differentially expressed copper metabolism-related genes (DE-CMRGs) were obtained from the overlap of CMRGs with DEGs, and the overlapped part was subjected to subsequent analysis.

Functional Enrichment Analyses

To gain further insights into the biological functions of the DEGs, we performed Gene Ontology (GO) enrichment analysis and Kyoto Encyclopedia of Genes and Genomes (KEGG) pathway analysis. These analyses were conducted in R using the "clusterProfiler" package.

Evaluating the Immune Cell Infiltration

The composition of the immunological microenvironment includes immunology cells, inflammatory cells, mesenchymal tissues, and various cytokines and chemokines. Analyzing the infiltration of immune cells plays a vital role in comprehending the progression of diseases and the response to treatments. To evaluate the immunological characteristics, a modified version of Gene Set Enrichment Analysis (GSEA), termed single sample gene set enrichment analysis (ssGSEA), was developed. This technique utilizes 23 immune gene sets and can be implemented using the "GSVA" R package.

Machine Learning

To refine the list of potential genes for DFU, we employed three machine learning techniques: Least Absolute Shrinkage and Selection Operator (LASSO) regression, Support Vector Machine (SVM), and Random Forest (RF). LASSO regression is a regularization technique that enhances prediction accuracy and model interpretability by selecting relevant variables and reducing model complexity. SVM is a powerful method used to establish a decision boundary between two classes, allowing for label prediction based on one or multiple feature vectors. RF, on the other hand, is a suitable technique for predicting continuous variables with minimal apparent fluctuations. It offers the advantages of not imposing constraints on variable conditions and providing high accuracy, sensitivity, and specificity. We performed LASSO regression, SVM, and RF analyses using the following R packages: "glmnet" for LASSO regression, "kernlab" for SVM, and "randomForest" for RF. The genes that intersected among these three techniques were considered as key CMRGs for DFU. To visualize the interaction between these central cuproptosis genes, we utilized the "circlize" R package. To further evaluate the predictive capacity of the DFU diagnosis model, we conducted receiver operating characteristic (ROC) analysis using the "pROC" R package. The ROC analysis helps assess the model's ability to discriminate between DFU and controls.

Quantitative Real-Time PCR (qRT-PCR)

During debridement treatment for DFU, the skin tissue removed from the edges of the wound is collected as the DFU group. Similarly, skin samples from the surface of acute traumatic lesions are collected as the acute wound group. Additionally, normal skin tissue collected from the margins of benign skin tumors, such as nevus, which are excised during surgery from healthy individuals. These samples were obtained from Zhongnan Hospital of Wuhan University. Written informed consents were secured from the patients or their family members. The study received approval from the Institutional Ethics Board and complies with the Declaration of Helsinki.

After tissue grinding, total RNA was extracted from tissue of human using Trizol Reagent (BIOLOGY, BOLG601). A total of 500 ng of RNA was used for complementary DNA synthesis using the All-in-one First-strand Synthesis MasterMix (BIOLOGY, BOLG10253). Real-time PCR reactions were performed using Taq SYBR Green qPCR Premix (iScience, EG20117M) in a total volume of 20ul, according to the manufacturer's protocol. The relative expression level of each messenger RNA (mRNA) of interest gene was normalised to the ACTB gene value and shown as the fold change relative to control. Real-time PCR primer sequences are shown in Supplementary Table 1.

Processing of Single-Cell RNA Sequencing (scRNA-Seq) Data

We accessed scRNA-seq data (GSE165816) of DFU consisting of five skin samples from subjects with non-healing ulcers from the GEO database and analyzed it using the "Seurat" and "harmony" packages. Cells with a percentage of mitochondrial genes higher than 15%, percentage of ribosome genes higher than 3%, percentage of erythrocyte genes less than 0.1%, cell counts less than three, or cells expressing greater than 7500 genes were excluded to retain high-quality data. The gene expression of the included cells was normalized using the "NormalizeData" function. We then performed a principal component analysis to extract the top 15 principal components based on the top 2000 highly variable genes,

which were retained for further analysis using the "FindVariableFeatures" function. To perform unsupervised and unbiased clustering of cell subpopulations, we applied the "FindNeighbors", "FindClusters" (resolution = 0.5), and "RunUMAP" functions. The "SingleR" package was used to annotate cell types. The marker genes for each cluster were screened by the 'FindAllMarkers' function. Finally, HALLMARK pathways were scored using the gene set variation analysis (GSVA) package, and the "irGSEA" package was used to score and integrate the differential gene sets.

Statistical Analysis

R version 4.2.2 was utilized for data analysis and statistical analyses. The Wilcoxon test was employed to determine the statistical distinction between the two groups. To examine the relationship between the expression levels of genes linked to copper metabolism and immune infiltration, a Spearman correlation was applied. Statistical analysis of qRT-PCR data involved assessing multiple group comparisons through one-way ANOVA, followed by Tukey's post hoc test. A p-value of 0.05 was considered to determine statistical significance.

Results

Merging GEO Data and Identification of DEGs

The integrated dataset consists of 42 DFU and 18 control samples and was obtained by removing the batch effects from the GEO dataset (Figure 1A and B). Using a volcano plot, we identified a total of 1928 DEGs (Figure 1C). The top 20 up and down-regulated genes between DFU patients and controls were visualized using a heat map (Figure 1D), suggesting their potential involvement in the pathological of DFU.

Functional and Pathway Enrichment Analysis of DEGs

We conducted a GO and KEGG enrichment pathway analysis in R to investigate the possible role of these DEGs. The GO enrichment analysis revealed energy metabolism, such as purine ribonucleotide metabolic process, energy derivation by oxidation of organic compounds, cellular respiration-aerobic respiration, respiratory electron transport chain, tricarboxylic acid cycle, mitochondrial protein-containing complex, tricarboxylic acid cycle enzyme complex. Moreover, we also demonstrated enrichment of electron transfer activity, oxidoreductase activity, NADH dehydrogenase (ubiquinone or quinone) activity, and NAD binding oxidoreductase activity (Figure 1E).

According to the KEGG analysis, DEGs were found to be enriched in pathways of neurodegeneration, involved multiple diseases, such as Alzheimer disease, Parkinson disease, Prion disease, Huntington disease, Diabetic cardiomyopathy. DEGs were found to be enriched in the following pathways according to the KEGG analysis: CGMP-PKG signaling pathway, AMPK signaling pathway, Thyroid hormone signaling pathway, Insulin signaling pathway, Adipocytokine signaling pathway. The KEGG analysis revealed an enrichment of DEGs in specific metabolic categories as followed: Carbon metabolism, Citrate cycle (TCA cycle), Glycolysis/Gluconeogenesis, Propanoate metabolism, Pyruvate metabolism, and Biosynthesis of amino acids, Valine, leucine and isoleucine degradation (Figure 1F).

Immune-Related Cell Landscape

Based on the ssGSEA algorithms described in the methods section, we observed an increased level of immune infiltration in the DFU group compared to the control, as demonstrated by the boxplot. Among the 23 immune cell subsets, immature B cells, macrophages, monocytes, and NK T cells showed differences between the DFU and control, with a notable decrease in the proportion of these four immune-related cells (Figure 2A). Furthermore, we observed strong positive correlations among almost all immune cells, except for Type 17 T helper cell and NK cells, which showed a negative correlation with other cells (Figure 2B). Diverse types of immune cells were infiltrated uniquely in DFU, which might serve as a possible therapeutic target for diabetic wound.

Identification of the Copper-Metabolism Signature via Machine Learning

Ten CMRGs were screened after the intersection of the 563 DEGs and 52 CMRGs (Figure 3A). And the overall expression of CMRGs between the DFU and the normal samples is shown in Figure 3B. What's more, most DE-CMRGs were expressed

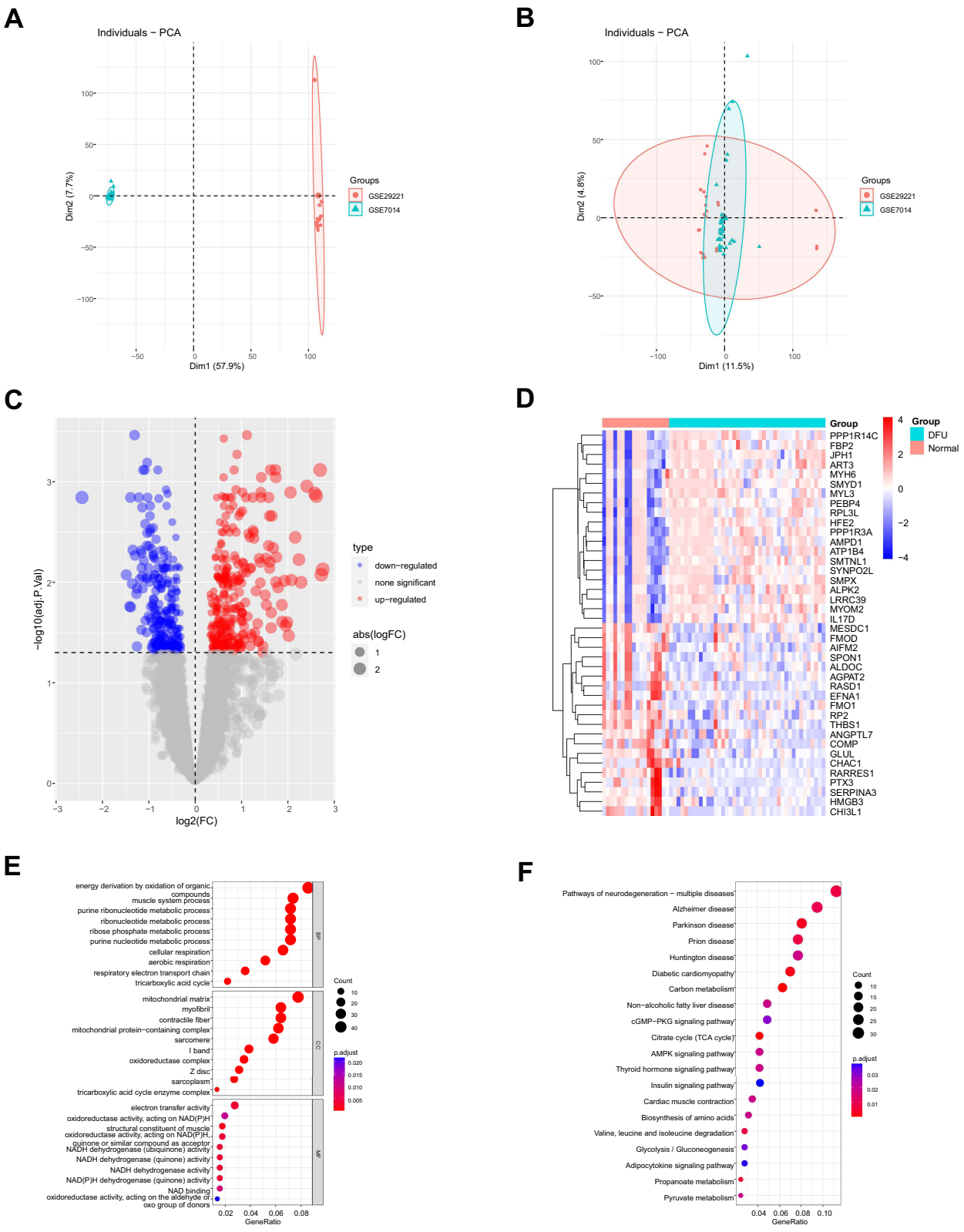

Figure 1 GEO Combined datasets and analysis of DEGs. (**A, B**) The PCA cluster plot of GSE29221 and GSE7014 before and after de-batching. (**C**) The volcano plot of DEGs between DFU and controls. (**D**) Clustered heatmap of DFU related DEG expression levels. (**E**) The GO analysis dot plot showed the enrichment of the DEGs. (**F**) Enriched items in KEGG pathway analysis. DFU, Diabetic Foot ulcers; DEGs, Differentially expressed genes; GO, Gene Ontology; KEGG, Kyoto Encyclopedia of Genes and Genomes.

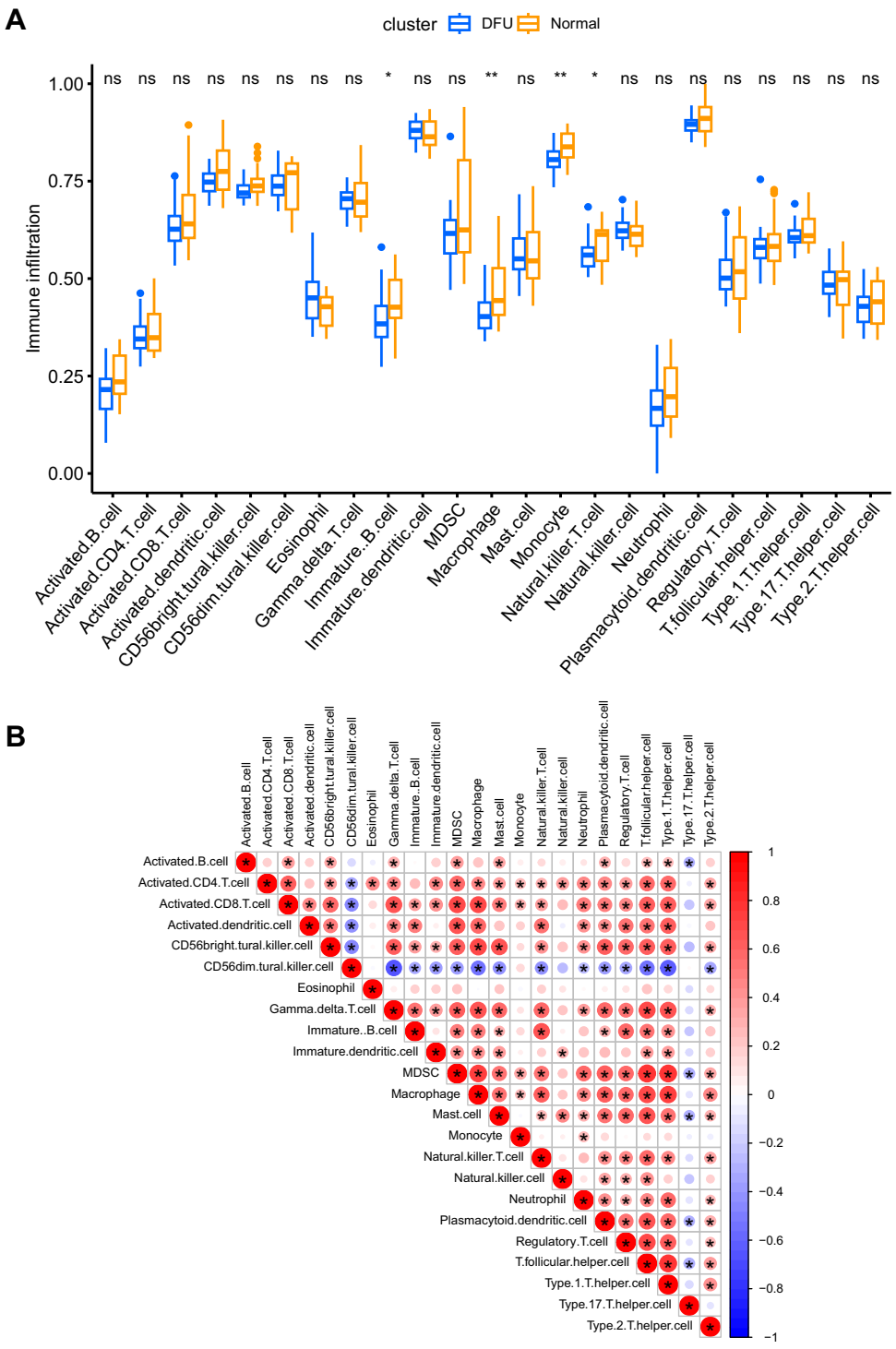

Figure 2 Immune cell infiltration analysis. (**A**) Box diagram for the comparison of 23 immune cell subtypes between DFU and control. (**B**) Correlation matrix of all 23 types of immune cell subtype compositions; size and color of the circle represent the Pearson correlation coefficients. ns, no significance; *p < 0.05, **p < 0.01.

at higher levels, except SLC31A1, MT1F, and HEPH. After obtaining DE-CMRGs, the LASSO regression technique, SVM, and random forest algorithms were utilized to screen potential genes for the construction of the cuproptosis-signature (Figure 4A–C). Finally, a three-gene cuproptosis-signature, including SLC31A1, ADNP, DLAT was identified (Figure 4D). As shown in Figure 4E, these three copper-metabolism-signature genes, are highly correlated with each other (Figure 4E). To predict DFU, the ROC curves of the three gene signatures were analyzed. Notably, DLAT had the highest AUC among the

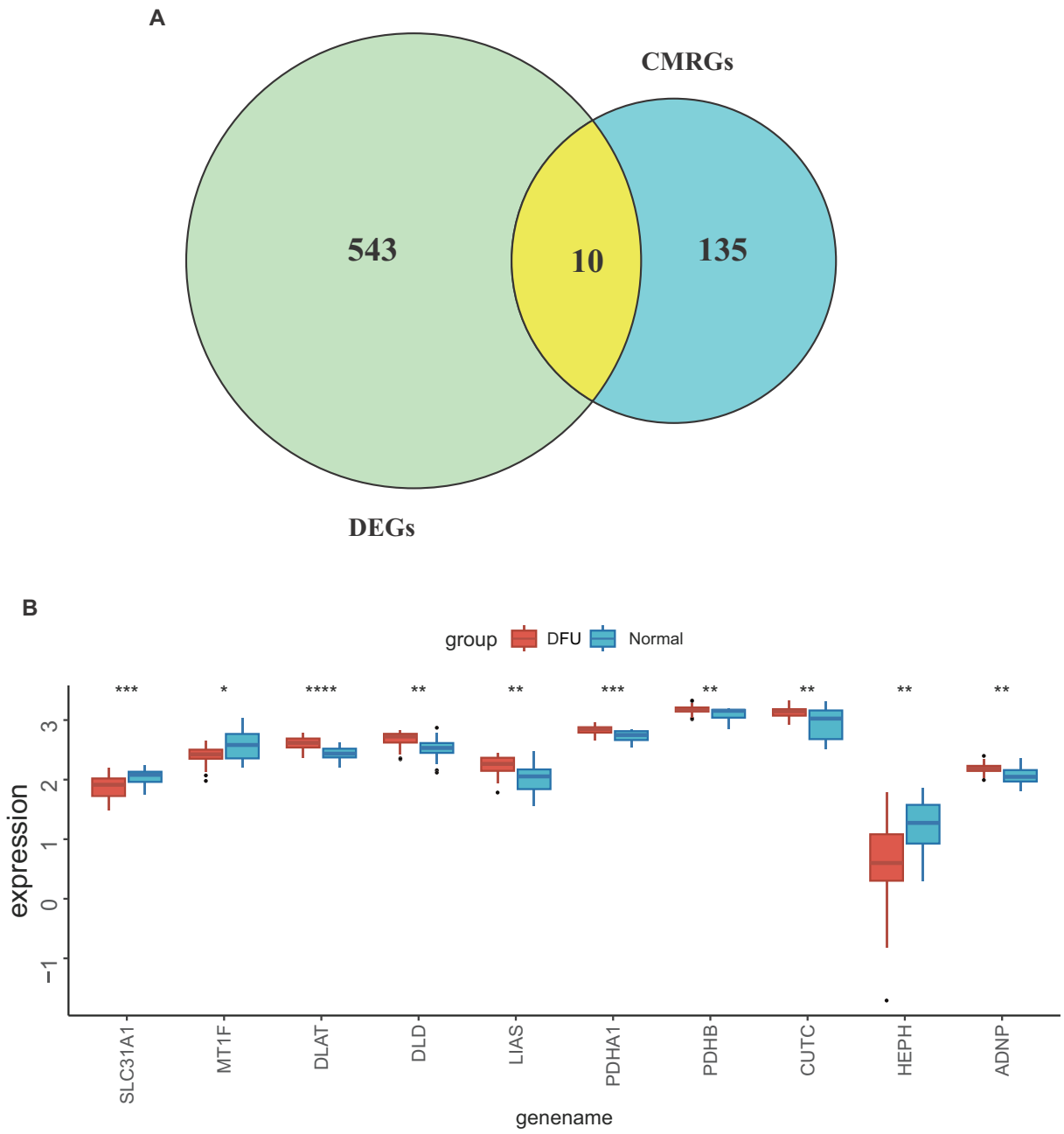

Figure 3 The candidate key DE-CMRGs in DFU. (**A**) The VennDiagram of the overlapped of genes between DEGs and CMRGs. (**B**) Overall expression histogram of candidate key DE-CMRGs in DFU. DEGs, Differentially expressed genes; CMRGs, copper metabolism-related genes; DE-CMRGs, differentially expressed copper metabolism-related genes. *p < 0.05; **p < 0.01; ***p < 0.001; ****P<0.0001.

three key genes, with a value of 0.832. Other AUC value for SLC31A1 and ADNP were 0.748, and 0.779, respectively (Figure 4F). These results indicated that these three gene signatures had excellent diagnostic value.

Immune Characteristics and ssGSEA of Key DE-CMRGs

Considering the importance of multiple immune components in the pathological mechanism of DFU, we analyzed the interrelation between immune cells and key DE-CMRGs in DFU (Figure 5A–C). For example, ADNP showed upregulated in immature dendritic cell, while downregulated in CD56bright natural killer cell. The SLC31A1 exhibited a strongly positive relationship with the infiltration of most immune cells, according to correlation analysis. And DLAT

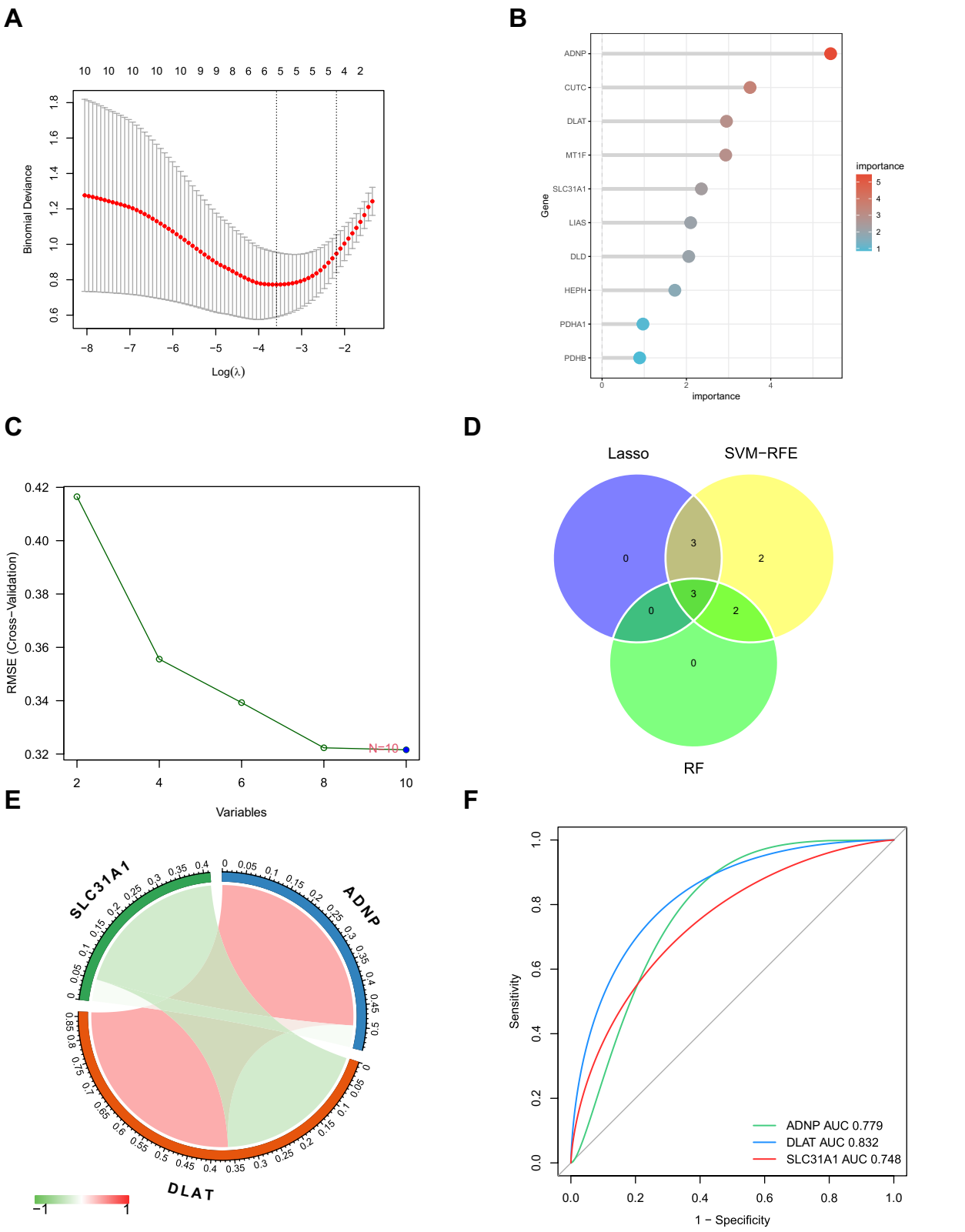

Figure 4 Identification of DE-CMRGs related signature. (**A-C**) Construction of DE-CMRGs signatures using LASSO regression, RF and SVM algorithm. (**D**) VennDiagram shows the overlap of candidate genes between the above three algorithms. (**E**) Circos plot displaying the relationship between the overlapping genes. (**F**) ROC curve of DE-CMRGs signatures in DFU diagnosis. DE-CMRGs, differentially expressed copper metabolism-related genes; LASSO, least absolute shrinkage and selection operator; SVM, support vector machine; RF, random forest; ROC, receiver operating characteristic.

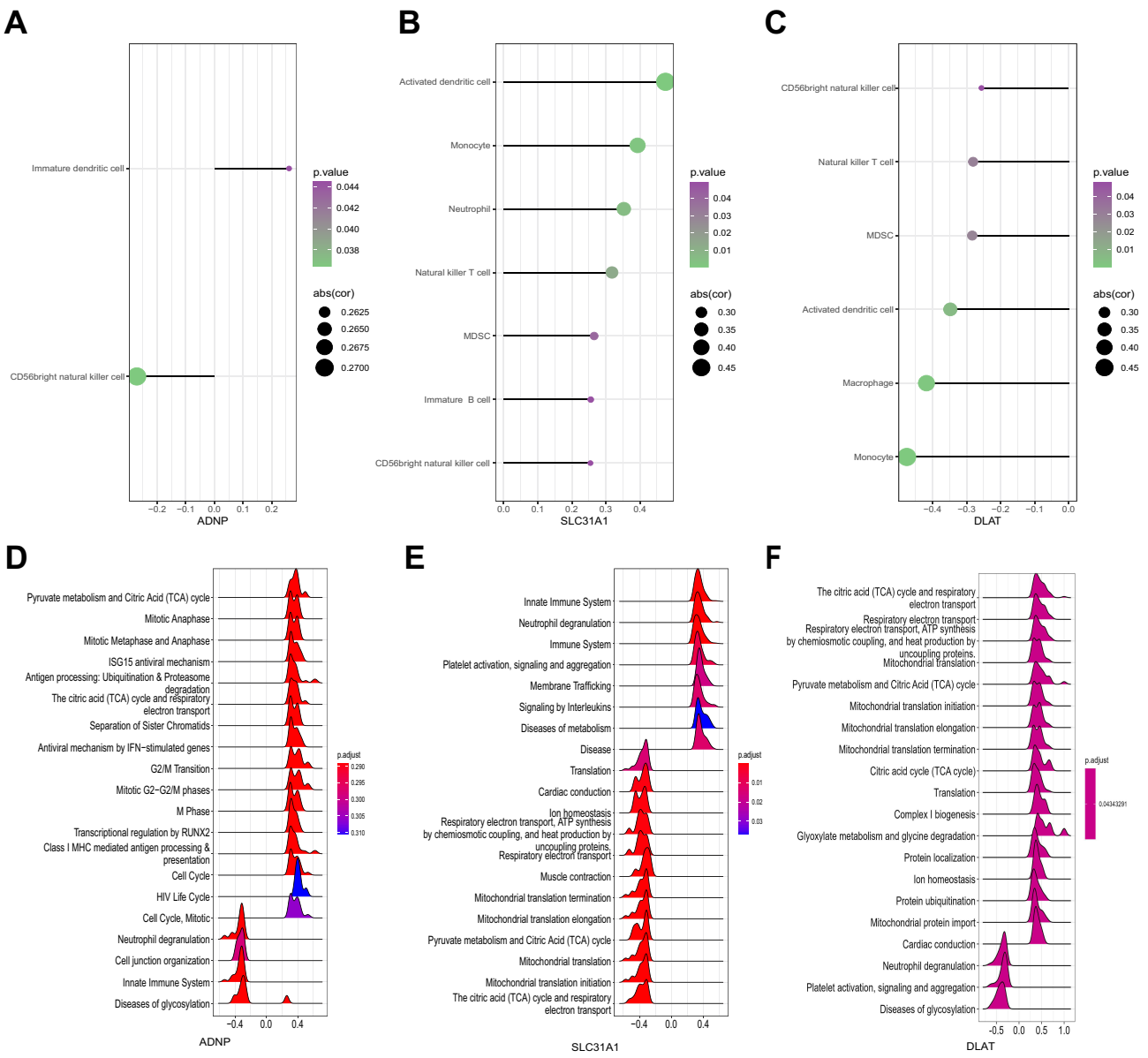

Figure 5 Correlations and pathway enrichment analysis for individual genes and immune cell infiltration. (**A-C**) The correlation between the infiltration levels of different immune cells and the expression of individual genes. (**D-F**) The Gene Set Enrichment Analysis (GSEA) results for ADNP, SLC31A1, and DLAT, highlighting the top 20 enriched Reactome pathways.

had a significantly negative relationship with 6 kinds of immune cells. SLC31A1, ADNP, DLAT were strongly enriched in metabolic and immune-related pathways (Figure 5D–F).

Correlated Genes Expression for DFU Tissues

DFU tissues were examined using qRT-PCR, compared with normal tissue and acute wound. The results showed that DLAT was not expressed, SLC31A1 was significantly downregulated in diabetic foot tissue, while ADNP was significantly upregulated (Figure 6A–B). These results were consistent with the predictions by machine learning algorithms.

Single-Cell Analysis Confirm the Relationship Between Copper Metabolism and DFU

Gene expression profiles of 15,462 cells from the five samples were obtained from the GSE165816 dataset. Supplementary Figure 1 illustrates the rationalization of sequencing depth, the number of detected genes, and the normalization of selected

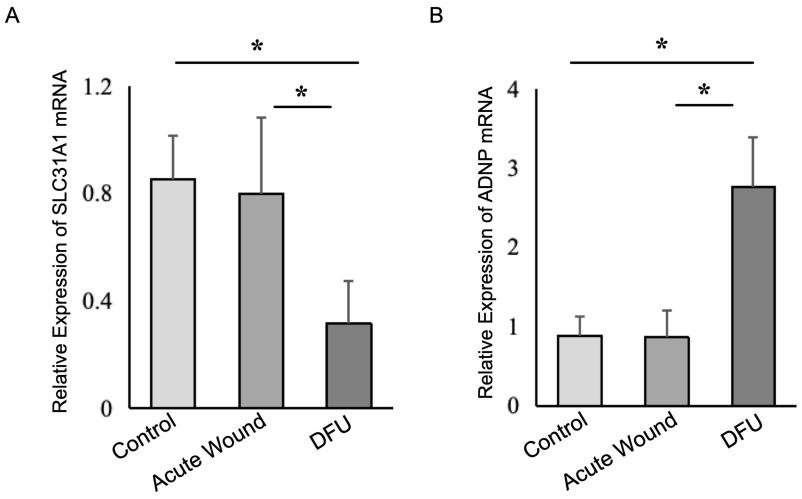

Figure 6 Real-time quantitative PCR was performed to measure SLC31A1 and ADNP. We collected 10 cases each of DFU and healthy control, along with 6 cases of acute traumatic wounds. (**A**) The expression differences of SLC31A1 among the control, acute wound, and DFU groups were analyzed using qRT-PCR. (**B**) The statistical differences of ADNP among the three groups by qRT-PCR. *P < 0.05.

data. We applied the "RunPCA" function to reduce dimensionality, resulting in the identification of 16 clusters (Figure 7A). Subsequently, the SingleR package was utilized to annotate and visualize the clustering of the downscaled cell types. In total, we identified ten major cell types in this step, namely fibroblasts, tissue stem cells, T cells, endothelial cells, keratinocytes, macrophages, epithelial cells, chondrocytes, monocytes, and neurons (Figure 7B and C). The heatmap presented the top five marker genes in these cell subpopulations (Figure 7D). Figure 8A depicted the distribution and expression of central genes across different cell types. SLC31A1 was found to be highly expressed in macrophages relative to other cell types, while ADNP exhibited high levels in fibroblasts and chondrocytes. Figure 8B displayed the expression levels of CMRGs in these cells, with chondrocytes exhibiting the highest scores, followed by fibroblasts and tissue stem cells. Subsequently, the cells were divided into high-score and low-score groups based on the relationship between individual expression and the mean expression within the cell class. Then we quantified the proportions of different cell types within these two groups and presented them in a bar chart (Figure 8C). Among them, fibroblasts and tissue stem cells accounted for a larger proportion in the high-score group. However, T cells accounted for a greater proportion of cells in the low-score group. Finally, the differentially enriched pathways between the two groups were analyzed by GSVA (Figure 8D). Interestingly, all 50 HALLMARK pathways were up-regulated in the high-score group.

Discussion

Currently, the treatment strategies for diabetic patients primarily focus on the resolution of superficial ulcers, but they often fall short in achieving complete control over the underlying metabolic pathology.[12] These strategies typically rely on the utilization of antibiotics, compression, debridement, pressure management, and specialized dressings.[12–14] Copper dressings or copper-based therapeutic approaches have surfaced as an effective method to improve the healing of ulcers, owing to copper's inherent antimicrobial properties, collagen cross linking and angiogenesis promotion, that may reduce infection risks, thereby facilitating further progress in healing. This suggests a significant link between copper metabolism and the pathophysiology of DFU. Hence, this research focuses on identifying genes associated with copper metabolism in DFU, with the objective of revealing potential therapeutic targets for intervention.

We analyzed gene expression levels in normal and diabetic wound samples using the GEO database and identified 563 DEGs. Our analysis also revealed an enrichment of electron transfer activity, specifically oxidoreductase activity, and NADH dehydrogenase activity. In diabetes patients, there is an alternate pathway for glucose metabolism that disrupts the balance between NADH and NAD+. The occurrence of such redox imbalance supports other pathways that lead to oxidative damage to DNA, lipids, and proteins and consequently to oxidative stress which further ascend diabetes and its complication.[15] DEGs analysis by KEGG revealed enrichment in various metabolic pathways. These pathways include

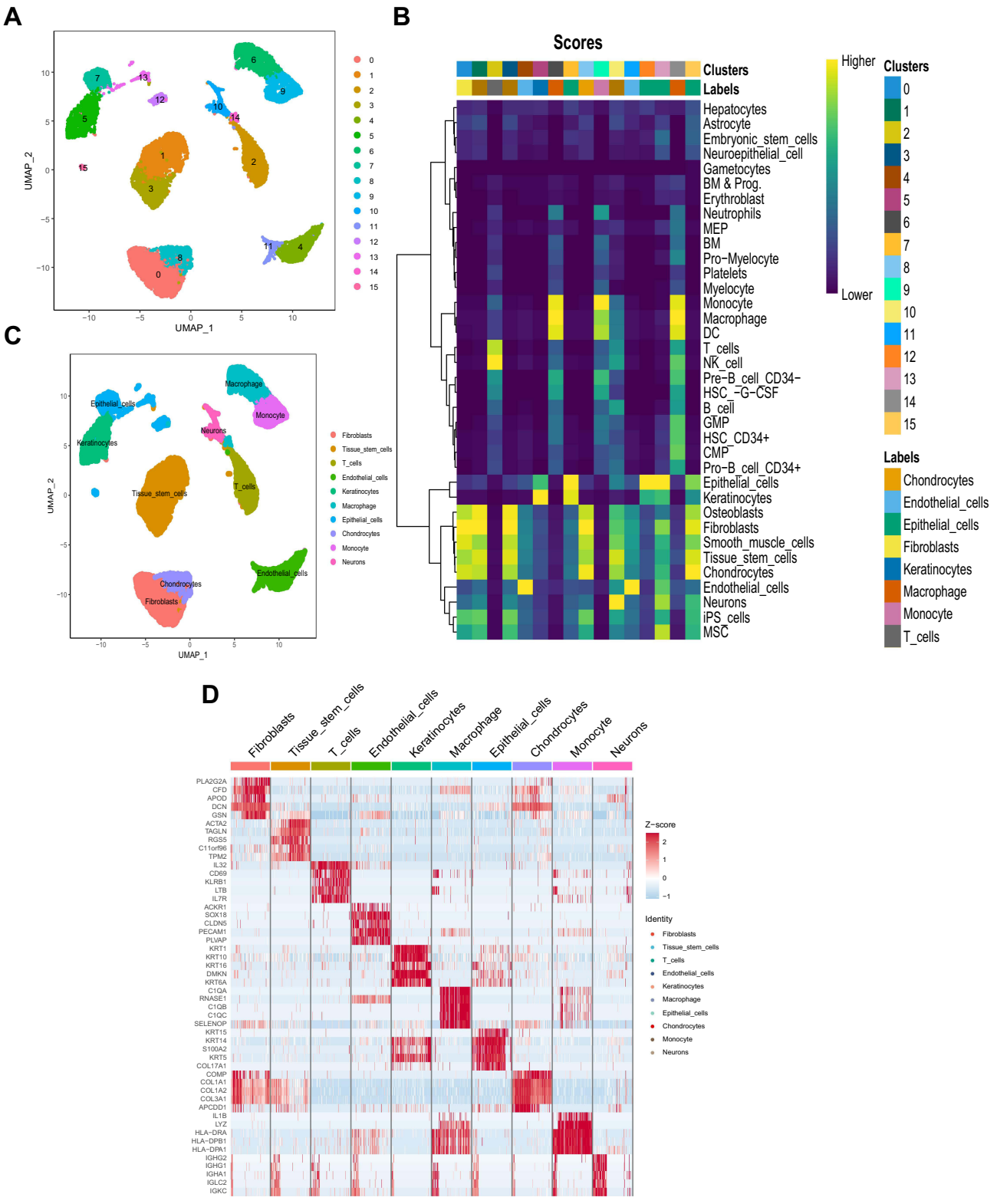

Figure 7 Analysis and Annotation of Single-Cell Sequencing Data. (**A**) Cells were clustered into 16 types using a UMAP plot. (**B, C**) The cells were then further divided into 10 distinct clusters using the SingleR algorithm and marker genes. (**D**) Heatmap displaying the expression of the top 5 marker genes among the 10 identified cell clusters.

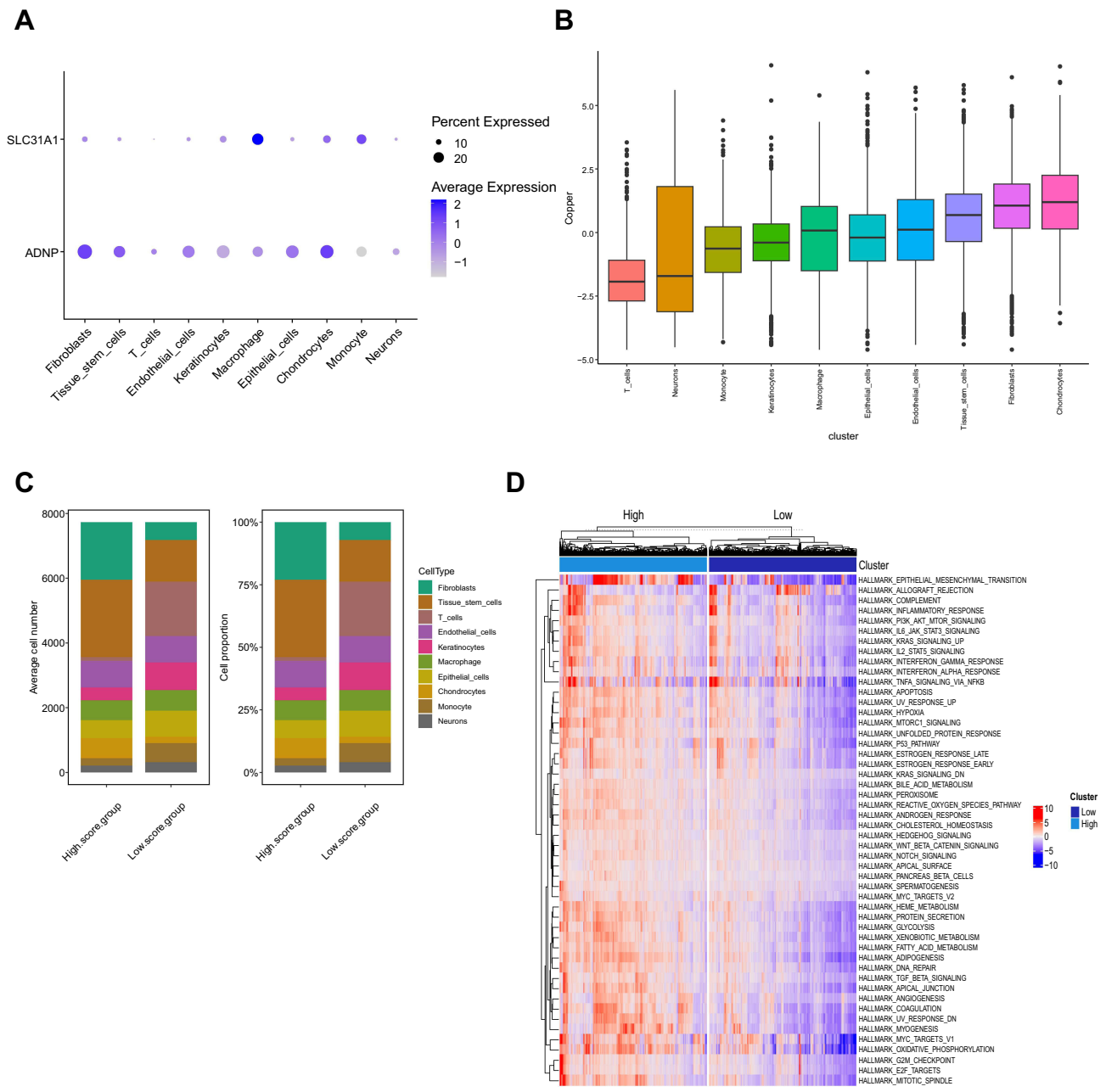

Figure 8 Copper metabolism analysis at the level of single-cell subpopulations. (**A**) Dot plots showing the distribution of two hub genes in various cell types. (**B**) Expression of gene sets related to copper metabolism in different cell types. (**C**) Average cell number and relative proportion of cell types in the groups with high and low copper metabolism scores. (**D**) Heatmap of differentially enriched pathways between the copper metabolism score high and low cells.

the production of amino acids, breakdown of valine, leucine, and isoleucine, energy production through glycolysis/gluconeogenesis, metabolism of propanoate, and breakdown of pyruvate.

Impaired amino acid metabolism, characterized by elevated levels of N-acetylaspartic acid, L-valine, isoleucine, asparagine, betaine, and L-methionine, plays a significant role in the onset and progression of both type 2 diabetes mellitus (T2DM) and diabetic kidney disease (DKD).[16] Recent studies suggest that high levels of branched chain amino acids (BCAAs), which include isoleucine, leucine, and valine, may contribute to the development of type 2 diabetes and obesity.[17] In the high-risk group of DFU, there was a notable increase in the number of genes involved in amino acid metabolism, along with higher levels of valine, leucine, and isoleucine degradation, as well as an increased presence of

pathways related to propanoate metabolism.[18] Efficient mitochondrial pyruvate metabolism is essential for facilitating the substantial influx of pyruvate into the gluconeogenic pathway, which is significantly elevated in diabetes.[19]

Through KEGG analysis, it was observed that DEGs were significantly associated with pathways related to neurodegenerative diseases, including Alzheimer's disease, Parkinson's disease, Prion disease, Huntington's disease, and Diabetic cardiomyopathy. Recent evidence has shown a correlation between energy metabolism and neurodegeneration, with T2DM increasing the risk of Alzheimer's disease, Parkinson's disease, Huntington's disease, and multiple sclerosis.[20–22] DEGs were found to be enriched in the following items according to the KEGG analysis: CGMP-PKG signaling pathway, AMPK signaling pathway, Thyroid hormone signaling pathway, Insulin signaling pathway, Adipocytokine signaling pathway. AMPK signaling has been found to enhance insulin sensitivity, offering potential treatment options for diabetic patients.[23] AMPK upregulation not only inhibits stress and cell death in β cells but also plays a crucial role in preventing the development of type 1 diabetes.[24] The protective effects of Ginsenoside Rb1 against diabetic cardiomyopathy involve the regulation of the adipocytokine pathway.[25]

The boxplot analysis revealed a higher prevalence of immature B cells, macrophages, monocytes, and NK cells among diabetic patients. Previous studies have shown that NK cells are significant in diabetic foot inflammation, while disease activity in diabetic foot is associated with macrophages.[26] A decrease in the frequency of NK cells plays a crucial role in the development of T2DM and its subsequent foot complications.[27] Chronic wounds, which are associated with dysregulated immune cells such as M1 macrophages, result from persistent inflammation and hinder the healing process of diabetic foot ulcers by disrupting the polarization of M2 macrophages.[28] The transition between classical and non-classical monocytes plays a crucial role in regulating inflammation and tissue repair during the healing of diabetic wounds.[29] This finding further emphasizes the significance of immune response in the development of diabetic foot.

After analyzing 563 DEGs and 52 genes related to copper metabolism, a total of 10 DE-CMRGs were identified. Our qRT-PCR analysis confirmed that SLC31A1 was downregulated and ADNP was upregulated in refractory DFU, consistent with the predicted data. SLC31A1 is a copper transporter that plays a role in maintaining copper balance. For diabetes, the accumulation of advanced glycosylation end products and copper leads to the upregulation of ATF3/SPI1/SLC31A1 signaling, disrupting copper balance and promoting cuproptosis.[30] Furthermore, in diabetic mice hearts model, an upregulation of SLC31A1 and alterations in cuproptosis-related protein expression were observed.[31] Low levels of ADNP transcripts may indicate a poorer response to stressful events, highlighting ADNP's significance in the stress response.[32] Pituitary adenylate cyclase-activating polypeptide (PACAP) has direct and indirect effects in diabetic retinopathy, activating related receptors and increasing the synthesis of activity-dependent neuroprotective protein (ADNP).[33] To explore ADNP's role and counteract deficiencies, a small peptide called NAP, containing an active site sequence of ADNP, was studied for its neuroprotective effect in diabetic retinopathy model.[34]

MT1F is downregulated in the colon tissues' normal-adenoma-carcinoma sequence.[35] The DLAT subunit of the pyruvate dehydrogenase complex is upregulated in gastric cancer and is considered a cuproptosis-related gene.[36] Inhibiting microbial CutC may be a potential therapeutic approach to reduce the risk of cardiovascular disease and thrombosis.[37] The α-ketoglutarate dehydrogenase complex (KGDC) is responsible for converting α-ketoglutarate to succinyl-coenzyme A in the Krebs cycle, and it consists of three subunits: E1 (encoded by PDHA1), E2 (encoded by DLST), and E3 (encoded by DLD).[38] At the molecular level, AMPK is found within the mitochondrial matrix and it phosphorylates the catalytic alpha subunit of PDHc (PDHA).[39] LIAS is responsible for encoding a protein belonging to the biotin and lipoic acid synthetases family, and this enzyme is specifically found in the mitochondrion.[40] The PDHB gene, which is involved in glycolysis, is regulated by the circadian clock and has been implicated in cancer progression and metastasis.[41] The HEPH gene belongs to a group of proteins called multicopper oxidases, and it may also play a role in maintaining copper balance and transport.[42] However, the relevance of these genes in DFU has not been documented and further research is required.

However, this study has several limitations that should be acknowledged. Firstly, our results require much more additional confirmation through rigorous and clinical trials. The findings are solely based on comprehensive bioinformatics analysis, utilizing data from a public database, which introduces the possibility of selection bias. Well-designed prospective studies are essential to validate our findings. The potential impact of this therapy on gene remains unknown. Further investigations are warranted to elucidate the underlying mechanisms involved.

Conclusions

This study utilized Bulk RNA-seq and scRNA-seq to investigate central genes and immune cell composition in DFU. Single-cell transcriptomic analysis unveiled the heterogeneity of DFU at the cellular level and its association with copper metabolism. Importantly, the study shows that regulating copper metabolism is a potential strategy in managing DFU and provides valuable information for future research.

Data Sharing Statement

The datasets presented in this study can be found in online repositories. The names of the repositories and accession number can be found in the article material.

Ethics Approval

Written informed consents were obtained from the patient or family members, and the study were approved by the Institutional Ethics Board of Zhongnan Hospital of Wuhan University (Wuhan, China).

Funding

This research received no external funding.

Disclosure

The authors declare no conflicts of interest in this work.

References

1. Patel S, Srivastava S, Singh MR, Singh D. Mechanistic insight into diabetic wounds: pathogenesis, molecular targets and treatment strategies to pace wound healing. *Biomed Pharmacother*. 2019;112:108615. doi:10.1016/j.biopha.2019.108615
2. Davis FM, Kimball A, Boniakowski A, Gallagher K. Dysfunctional wound healing in diabetic foot ulcers: new crossroads. *Curr Diab Rep*. 2018;18(1):2. doi:10.1007/s11892-018-0970-z
3. Reardon R, Simring D, Kim B, Mortensen J, Williams D, Leslie A. The diabetic foot ulcer. *Austra J Gener Pract*. 2020;49(5):250–255. doi:10.31128/AJGP-11-19-5161
4. Tsvetkov P, Coy S, Petrova B, et al. Copper induces cell death by targeting lipoylated TCA cycle proteins. *Science*. 2022;375(6586):1254–1261. doi:10.1126/science.abf0529
5. Li SR, Bu LL, Cai L. Cuproptosis: lipoylated TCA cycle proteins-mediated novel cell death pathway. *Signal Trans Targe Thera*. 2022;7(1):158. doi:10.1038/s41392-022-01014-x
6. Chen X, Cai Q, Liang R, et al. Copper homeostasis and copper-induced cell death in the pathogenesis of cardiovascular disease and therapeutic strategies. *Cell Death Dis*. 2023;14(2):105. doi:10.1038/s41419-023-05639-w
7. Oliveri V. Biomedical applications of copper ionophores. *Coord Chem Rev*. 2020;422:213474. doi:10.1016/j.ccr.2020.213474
8. Yadav C, Srikantiah RM, Manjrekar P, Shenoy MT, Chaudhury D. Assessment of mineral pathophysiology in patients with diabetic foot ulcer. *Biol Trace Elem Res*. 2020;195(2):366–372. doi:10.1007/s12011-019-01868-3
9. Chang W, Li P. Copper and diabetes: current research and prospect. *Mol Nutr Food Res*. 2023;67(23):2300468. doi:10.1002/mnfr.202300468
10. Zhang R, Jiang G, Gao Q, et al. Sprayed copper peroxide nanodots for accelerating wound healing in a multidrug-resistant bacteria infected diabetic ulcer. *Nanoscale*. 2021;13(37):15937–15951. doi:10.1039/D1NR04687J
11. Xiao J, Chen S, Yi J, Zhang HF, Ameer GA. A cooperative copper metal–organic framework-hydrogel system improves wound healing in diabetes. *Adv Funct Mater*. 2017;27(1):1604872. doi:10.1002/adfm.201604872
12. Ahmed R, Augustine R, Chaudhry M, et al. Nitric oxide-releasing biomaterials for promoting wound healing in impaired diabetic wounds: state of the art and recent trends. *Biomed Pharmacother*. 2022;149:112707. doi:10.1016/j.biopha.2022.112707
13. Chang M, Nguyen TT. Strategy for treatment of infected diabetic foot ulcers. *Acc Chem Res*. 2021;54(5):1080–1093. doi:10.1021/acs.accounts.0c00864
14. Kolimi P, Narala S, Nyavanandi D, Youssef AA, Dudhipala N. Innovative treatment strategies to accelerate wound healing: trajectory and recent advancements. *Cells*. 2022;11(15):2439. doi:10.3390/cells11152439
15. Garg SS, Gupta J. Polyol pathway and redox balance in diabetes. *Pharmacol Res*. 2022;22:106326. doi:10.1016/j.phrs.2022.106326
16. Zhu H, Bai M, Xie X, et al. Impaired amino acid metabolism and its correlation with diabetic kidney disease progression in type 2 diabetes mellitus. *Nutrients*. 2022;14(16):3345. doi:10.3390/nu14163345
17. Ramzan I, Ardavani A, Vanweert F, Mellett A, Atherton PJ, Idris I. The association between circulating branched chain amino acids and the temporal risk of developing type 2 diabetes mellitus: a systematic review & meta-analysis. *Nutrients*. 2022;14(20):4411. doi:10.3390/nu14204411
18. Zhang S, Li S, Huang J, et al. Gram-negative bacteria and lipopolysaccharides as risk factors for the occurrence of diabetic foot. *J Clin Endocrinol Metab*. 2023;28:dgad178.
19. Ferguson D, Eichler SJ, Yiew NK, et al. Mitochondrial pyruvate carrier inhibition initiates metabolic crosstalk to stimulate branched chain amino acid catabolism. *Mol Metabol*. 2023;70:101694. doi:10.1016/j.molmet.2023.101694

20. Xxxx S, Ahmad MH, Rani L, Mondal AC. Convergent molecular pathways in type 2 diabetes mellitus and parkinson's disease: insights into mechanisms and pathological consequences. *Mole neuro*. 2022;59(7):4466–4487. doi:10.1007/s12035-022-02867-7
21. Onaolapo AY, Ojo FO, Adeleye OO, Falade J, Onaolapo OJ. Diabetes mellitus and energy dysmetabolism in Alzheimer's disease: understanding the relationships and potential therapeutic targets. *Current Diabetes Rev*. 2023;19(8):31–45. doi:10.2174/1573399819666230102141154
22. Michailidis M, Moraitou D, Tata DA, Kalinderi K, Papamitsou T, Papaliagkas V. Alzheimer's disease as type 3 diabetes: common pathophysiological mechanisms between Alzheimer's disease and type 2 diabetes. *Int J Mol Sci*. 2022;23(5):2687. doi:10.3390/ijms23052687
23. Entezari M, Hashemi D, Taheriazam A, et al. AMPK signaling in diabetes mellitus, insulin resistance and diabetic complications: a pre-clinical and clinical investigation. *Biomed Pharmacother*. 2022;146:112563.
24. Lu M, Wang Y, Jiang Y, et al. Berberine inhibits gluconeogenesis in spontaneous diabetic rats by regulating the AKT/MAPK/NO/cGMP/PKG signaling pathway. *Mol Cell Biochem*. 2023;4:1–5.
25. Zhang C, Han M, Zhang X, Tong H, Sun X, Sun G. Ginsenoside Rb1 protects against diabetic cardiomyopathy by regulating the adipocytokine pathway. *J Inflamm Res*. 2022;1:71–83. doi:10.2147/JIR.S348866
26. Rehak L, Giurato L, Meloni M, Panunzi A, Manti GM, Uccioli L. The immune-centric revolution in the diabetic foot: monocytes and lymphocytes role in wound healing and tissue regeneration—a narrative review. *J Clin Med*. 2022;11(3):889. doi:10.3390/jcm11030889
27. Hammad R, Elmadbouly AA, Ahmad IH, et al. T-natural killers and interferon gamma/interleukin 4 in augmentation of infection in foot ulcer in type 2 diabetes. *Diab Meta Synd Obes*. 2021;29:1897–1908. doi:10.2147/DMSO.S305511
28. Lin CW, Hung CM, Chen WJ, et al. New horizons of macrophage immunomodulation in the healing of diabetic foot ulcers. *Pharmaceutics*. 2022;14(10):2065. doi:10.3390/pharmaceutics14102065
29. Min D, Nube V, Tao A, et al. Monocyte phenotype as a predictive marker for wound healing in diabetes-related foot ulcers. *J diabet complicat*. 2021;35(5):107889. doi:10.1016/j.jdiacomp.2021.107889
30. Huo S, Wang Q, Shi W, et al. ATF3/SPI1/SLC31A1 signaling promotes cuproptosis induced by advanced glycosylation end products in diabetic myocardial injury. *Int J Mol Sci*. 2023;24(2):1667. doi:10.3390/ijms24021667
31. Wu G, Peng H, Tang M, et al. ZNF711 down-regulation promotes CISPLATIN resistance in epithelial ovarian cancer via interacting with JHDM2A and suppressing SLC31A1 expression. *EBioMedicine*. 2021;71:103558. doi:10.1016/j.ebiom.2021.103558
32. D'Amico AG, Maugeri G, Musumeci G, Reglodi D, D'Agata V. PACAP and NAP: effect of two functionally related peptides in diabetic retinopathy. *J Mol Neurosci*. 2021;1:1.
33. Scuderi S, D'Amico AG, Castorina A, et al. Davunetide (NAP) protects the retina against early diabetic injury by reducing apoptotic death. *J Mol Neurosci*. 2014;54(3):395–404. doi:10.1007/s12031-014-0244-4
34. Sragovich S, Ziv Y, Vaisvaser S, Shomron N, Hendler T, Gozes I. The autism-mutated ADNP plays a key role in stress response. *Transl Psychiatry*. 2019;9(1):235. doi:10.1038/s41398-019-0569-4
35. Yan DW, Fan JW, Yu ZH, et al. Downregulation of metallothionein 1F, a putative oncosuppressor, by loss of heterozygosity in colon cancer tissue. *Bioch Biophy Acta Molec Bas Dis*. 2012;1822(6):918–926. doi:10.1016/j.bbadis.2012.02.021
36. Goh WQ, Ow GS, Kuznetsov VA, Chong S, Lim YP. DLAT subunit of the pyruvate dehydrogenase complex is upregulated in gastric cancer-implications in cancer therapy. *Am J Transl Res*. 2015;7(6):1140.
37. Skye SM, Zhu W, Romano KA, et al. Microbial transplantation with human gut commensals containing CutC is sufficient to transmit enhanced platelet reactivity and thrombosis potential. *Circula res*. 2018;123(10):1164–1176. doi:10.1161/CIRCRESAHA.118.313142
38. Odièvre MH, Chretien D, Munnich A, et al. A novel mutation in the dihydrolipoamide dehydrogenase E3 subunit gene (DLD) resulting in an atypical form of α-ketoglutarate dehydrogenase deficiency. *Human Mutation*. 2005;25(3):323–324. doi:10.1002/humu.9319
39. Cai Z, Li CF, Han F, et al. Phosphorylation of PDHA by AMPK drives TCA cycle to promote cancer metastasis. *Molecular Cell*. 2020;80(2):263–278. doi:10.1016/j.molcel.2020.09.018
40. Cronan JE. Biotin and lipoic acid: synthesis, attachment, and regulation. *EcoSal Plus*. 2014;6(1):10–128. doi:10.1128/ecosalplus.esp-0001-2012
41. Wang G, Ye Q, Ning S, et al. LncRNA MEG3 promotes endoplasmic reticulum stress and suppresses proliferation and invasion of colorectal carcinoma cells through the MEG3/miR-103a-3p/PDHB ceRNA pathway. *Neoplasma*. 2020;68(2):362–374. doi:10.4149/neo_2020_200813N858
42. Kipen VN, Ivanova EV, Snytkov EV, Verchuk AN. Analysis of HEPH gene polymorphism on the x chromosome for identification of wild boar and domestic pig. *Russian J Genet*. 2020;56(9):1099–1108. doi:10.1134/S1022795420080062